Journal of Environmental Management 232 (2019) 1037–1048

Contents lists available at ScienceDirect

Journal of Environmental Management

journal homepage: www.elsevier.com/locate/jenvman

Research article

Characterization of elevation and land cover dependent trends of NDVI variations in the Hexi region, northwest China

Jing-Cheng Han[a], Yuefei Huang[a,b,c,*], Hua Zhang[d], Xiaofeng Wu[a]

[a] Water Research Center, Graduate School at Shenzhen, Tsinghua University, Shenzhen, 518055, China
[b] State Key Laboratory of Hydroscience & Engineering, Department of Hydraulic Engineering, Tsinghua University, Beijing, 100084, China
[c] State Key Laboratory of Plateau Ecology and Agriculture, Qinghai University, Xining, 810016, China
[d] School of Engineering and Computing Sciences, College of Science and Engineering, Texas A&M University — Corpus Christi, Corpus Christi, TX, 78412, USA

ARTICLE INFO

Keywords:
NDVI trend
Climate change
Elevation
Land cover
Precipitation
Temperature

ABSTRACT

In the arid Hexi Corridor of northwest China, vegetation cover plays a pivotal role in sustaining the unique terrestrial ecosystem. In this paper, vegetation changes during growth season from April to October were investigated through examining the trends in the Normalized Difference Vegetation Index (NDVI) across the Hexi region. Based on the GMMIS NDVI 3g.v1 dataset, NDVI trend and its dependency on elevation and land cover were analyzed for the period 1982–2015 according to multiple statistical tests. Results showed that NDVI exhibited a significantly increasing trend in ~70% of the vegetated area, in contrast with a negative trend only in 2.85%. The resulting distinct groups with respect to decreasing, increasing and no trends presented significant differences in elevation and land cover composition, and the correlation between elevation, land cover and NDVI trend magnitude was subjected to precipitation and temperature change. The elevation and grassland cover were found to mainly account for variations in NDVI trend, and increase in elevation and various types of land cover excluding impervious and bare land would facilitate the trend magnitude. The dependency of NDVI trend on elevation and land cover was very vulnerable to increasing air temperature, which triggered an improvement in the vegetable activity to adapt to climate change, especially grass and forest. The contribution of crop and shrub to NDVI change was sensitive to precipitation trend change, but the crop was primarily influenced by human activities. The identified patterns of vegetation change would help to gain insights into the adapting mechanism of the fragile ecosystems in arid areas to changing environmental conditions.

1. Introduction

Assessing how the distribution and dynamics of vegetation changes in response to varying environmental conditions has been increasingly important for ecologists to better predict the effects of global warming and human activity on terrestrial ecosystem functioning (Pettorelli et al., 2005). However, these efforts were seriously hampered by rather limited information about vegetation at large spatial and temporal scales. Fortunately, rapid development of remote sensing techniques resolved this dilemma, and it has been well revealed that a consistent correlation occurs between the Normalized Difference Vegetation Index (NDVI) and vegetation biomass and dynamics (Jackson and Huete, 1991; Myneni et al., 1995). Accordingly, NDVI has been the most widely used vegetation index in global ecological studies (Murray et al., 2013; Reed et al., 2009; Wang et al., 2015). In addition, NDVI has been considered to be the first useful tool to couple climate, vegetation and animal distribution and performance (Pettorelli et al., 2005). The NDVI data have been extensively acquired by satellite sensors (Zheng et al., 2018). However, the resulting uncertainties of NDVI would be highly associated with the study area as well as the chosen datasets for analysis due to various spatial-temporal resolutions and temporal coverages.

Vegetation changes in northwest China are always the major focus since arid/semi-arid region is one of the most sensitive and important areas to global changes due to its fragile ecosystems and desertification (Piao et al., 2010; Zhao et al., 2011, 2012). Regardless of data sources with different time lengths employed in these regions, previous studies generally summarized a significantly positive trend of vegetation growth in northwest China (Peng et al., 2011; Yang et al., 2016; Zhang et al., 2016; Zhao et al., 2012). Moreover, the relations between NDVI and climatic variables have been also examined broadly to make predictions viable and efficient (Hermance et al., 2015; Moreno-de las Heras et al., 2015; Zheng et al., 2018), but inconsistent results were

* Corresponding author. State Key Laboratory of Hydroscience and Engineering, Dept. of Hydraulic Engineering, Tsinghua Univ., Beijing, 100084, China.
E-mail addresses: han.jingcheng@sz.tsinghua.edu.cn (J.-C. Han), yuefeihuang@tsinghua.edu.cn (Y. Huang).

https://doi.org/10.1016/j.jenvman.2018.11.069
Received 26 June 2018; Received in revised form 13 November 2018; Accepted 16 November 2018
Available online 21 December 2018
0301-4797/

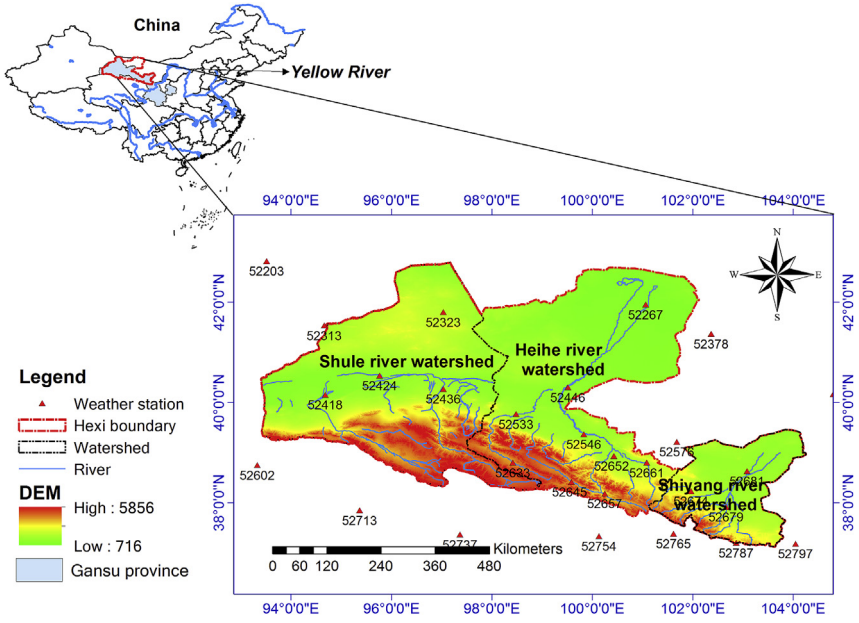

Fig. 1. Location of the Hexi region and weather stations.

obtained with respect to the correlation between vegetation change and precipitation and temperature (Yang et al., 2016). Nonetheless, the detected trends of vegetation were generally attributed to precipitation rather than temperature (Fang et al., 2013; Shi et al., 2007; Zhang et al., 2016; Zhao et al., 2011).

The Hexi region of northwest China comprises of three major endorheic river watersheds with a typical gravel desert ecosystem, and has experienced long history of human activities (Wang et al., 2003). Climate variations have caused serious threats to the ecological environment, vegetation growth, water and land resources in recent years (Zeng et al., 2018). Wei et al. (2018) concluded that climate change signal in the Pan-Hexi region appeared to be well correlated with the global climate change signal for the period 1960–2014, but the warming rate of the mean annual air temperature was significantly higher than that in China and the rest of the world. As far as we know, vegetation change in the arid region of northwest China was mostly investigated at a larger or local scale, and the impact of specific factors such as climate change (Gao and Zhang, 2016), desertification (Yang et al., 2016), water resource management (Yin et al., 2015) and sparse alpine vegetation (Zeng et al., 2018) was mainly the focus of previous studies. However, spatial analysis of inner vegetation change, its change rate and driving factors in the Hexi region is still lacking (Guan et al., 2018). According to Yang et al. (2016), vegetation was significantly improved in lower reaches of the inland river watersheds, and it was precipitation that mainly affected desert vegetation growth across the Hexi region. The identified areas with non-significant correlation between NDVI and annual precipitation were considered to be mainly influenced by human activities. In the contrast, precipitation was not a comparative factor for desert vegetation growth in the western arid watershed (Yang et al., 2016). The unique Gobi desert-oasis landscape and geomorphological features would render underlying surface conditions profound for vegetation changes, but to the authors' knowledge, few studies have been emphasized on the impacts of elevation and land cover types on the trend in vegetation changes as well as its association with climatic variables. Tao et al. (2015) found a more significant correlation between climate change and grassland vegetation variation in higher elevation areas of the Qinghai-Xizang Plateau. In this regard, it entails in depth analysis of spatial patterns of vegetation change to better understand trends in NDVI related to spatially heterogeneous conditions (Suding et al., 2015; Tao et al., 2015). Regardless of studies on the response of vegetation growth to climatic factors, the correlation between NDVI trend and precipitation and temperature change was not effectively investigated. Lack of knowledge of vegetation change due to climate change would also make it necessary to conduct complementary studies (Liu et al., 2015).

Through using NDVI as an indicator of vegetation cover, this study aims to determine the vegetation change trend dependent on land cover and elevation in the vegetated area of the Hexi region. To better represent the temporal and spatial features of vegetation change, trend analysis on NDVI change was performed at both the pixel and regional levels. In the meanwhile, land cover and elevation with fine resolution available were employed to characterize the dependency of NDVI trend based on multiple statistical tests and correlation analysis. Besides, the roles of precipitation and temperature change in affecting the correlation between NDVI trend and elevation and land cover were also analyzed and discussed in order to reflect the significant influences of climate change on vegetation growth.

2. Materials and methods

2.1. Study area

The Hexi region (37°17′~42°48′N, 93°23′~104°12′E) is mainly located in the northwest of the Yellow river basin, and the Hexi corridor, extending over 1000 km from east to west and 100–200 km from south to north, had played a key role in promoting worldwide communications as the most important route of the historic Silk Road from China to Central and Western Asia. As shown in Fig. 1, the study area consists of three inland river watersheds, and covers an area of 298,550.4 km^2 (129,335.8, 128,616.0 and 40,578.6 km^2 for the Shule, Heihe and Shiyang river watershed, respectively). The major rivers in the watersheds originate as the meltwater and precipitation of Qilian Mountains, and provide continuous flows for downstream utilization, sustaining very fragile ecosystem and development of regional industrial and agricultural economy (Zhang et al., 2015). These rivers finally disappear in the Gobi Desert as a result of infiltration, evaporation and irrigation consumptions, etc. The stream drought and precipitation in the Hexi region have been experiencing an increasing trend during last five decades, and the uneven spatial variations of precipitation, temperature and glacier runoff led to the difference of hydrological drought variations between the Shule, Heihe and Shiyang River basins (Gao and Zhang, 2016).

The Hexi region bears a typical continental arid climate with low precipitation, strong evapotranspiration, and dramatic temperature variability. According to daily weather observations during 1982–2015, the ranges of annual precipitation and annual average temperature across the region are 106 ~ 365 mm and 5.8–9.5 °C, respectively. Besides, remarkable variations exist in both precipitation and temperature among stations. For instance, annual average precipitation observed at Qilian station is 365 mm (52657 in Fig. 1) in comparison with 36.8 mm at Dunhuang station (52418 in Fig. 1). In addition to spatial variations, intra-annual precipitation also exhibits high variability, and there are notable differences in monthly precipitation during one year. Besides, almost 60% of the total precipitation amount occurs in summer.

Accounting for ~60% of Gansu Province, the Hexi corridor comprises nineteen agricultural counties and serves as the transportation hub and grain base of arid inland area in northwest China. The total area is resided by almost five million populations, 80% of which are farmers. Diverse landscapes can be found, such as alluvial and fluvial plains, shallow mountains, oases, deserts and Gobi, but they would be very sensitive to changing environmental conditions. Moreover, this region suffers from severe water shortage, and has experienced prominent water related issues such as ecological degradation, which has become the primary bottleneck for sustainable development (Zhang et al., 2015). Consequently, how to better regulate and restore the ecosystems has always been emphasized by the local government as well as the entire country (Wang et al., 2013).

2.2. Data sources and preprocessing

2.2.1. Elevation and climate data

The elevation raster data at 30 m spatial resolution were extracted from the Advanced Spaceborne Thermal Emission and Reflection Radiometer Global Digital Elevation Model Version 2 (ASTER GDEM V2) jointly released by the Ministry of Economy, Trade, and Industry (METI) of Japan and the United States National Aeronautics and Space Administration (NASA) and available from October, 2011. Monthly air temperature and precipitation records for the period from 1982 to 2015 at twenty eight individual weather stations (Fig. 1) based on daily observations were obtained from the Data Sharing Service System of China National Meteorological Administration (http://data.cma.cn/). Through using the ordinary Kriging method (Delhomme, 1978), spatial interpolation of monthly temperature and precipitation was further imposed on the entire region to produce a series of 0.0833°×0.0833° grids (1/12° resolution) with a geographical information processing software.

2.2.2. High-resolution land cover dataset

The land cover data were derived from the FROM-GLC-agg version (Finer Resolution Observation and Monitoring of Global Land Cover-Aggregation) of 30 m global land characterization dataset (http://data.ess.tsinghua.edu.cn/), which is an improved global land cover map through aggregating two kinds of 30 m resolution circa 2010 global land cover maps with two coarser resolution global maps, i.e., Nighttime Light Impervious Surface Area (NL-ISA) and MODIS urban extent (MODIS-urban) (Gong et al., 2013; Yu et al., 2014). As illustrated in Fig. 2a, ten types of land cover were delineated across the Hexi region from the global land cover dataset based on 91433 training samples and 38664 test samples collected via human interpretation of TM/ETM + images. Considering the study area mainly occupied by grassland, bare land, cropland, shrub, forest and impervious land, only six types of land cover were investigated in this study. Regarding the high-resolution land cover data, there are no time series of land cover maps available for the study area (Gong et al., 2013). Thus, land cover changes for the study period would not be recognized, and six types of land cover were roughly categorized in order to mask the transformations between various types of land cover.

2.2.3. NDVI data

The 15-day Global Inventory Modeling and Mapping Studies (GMMIS) NDVI dataset at 1/12° resolution (~8 km), generated from NOAA's Advanced Very High Resolution Radiometer (AVHRR) data, has been widely used for investigating long term vegetation dynamics at regional and global scales (Yang et al., 2016). The latest version 3g.v1 time series for the period through July 1981 to December 2015 are further improved by accounting for various deleterious effects and noises (https://ecocast.arc.nasa.gov/data). Regardless of relatively coarse resolution, the GMMIS NDVI 3g.v1 dataset has advantages of long time series and small uncertainty. Based on the datasets, monthly NDVI value was obtained using the Maximum Value Composite method (MVC), which assigns the maximum value in one month as the monthly NDVI value at each pixel. Fig. 2b shows the distribution of annual average NDVI values, and it could be observed that the NDVI value at a pixel is closely related to composition of land cover through comparing Fig. 2a with Fig. 2b. Taking vegetation cover into consideration, area with NDVI value smaller than 0.1 is masked as no vegetation, and only 25.5% of the Hexi region was identified as non-vegetation area (Fig. 3). Table 1 presents the area percentages of land cover types in three watersheds as well as corresponding average elevation. The main vegetation cover is grassland, the area proportion of which together with shrub, crop and forest increases from west to east. Since vegetation growth was the concern, only NDVI during growing period from April to October was considered in this study.

2.3. Methodology

Multiple tests and analysis methods were employed to reflect the characteristics of NDVI trend dependent on elevation and land cover. Firstly, seasonal Mann-Kendall (SMK) test was applied to detect the change trend with seasonality in NDVI during vegetation growth period, while the Sen's slope (SS) is used to analyze change magnitude of NDVI at pixel level. Subsequently, trend analysis of NDVI variations would be performed through demonstrating the spatial distribution of statistical significance and change magnitude across the Hexi region. With regards to NDVI trend change at pixels, land cover or elevation feature of pixels associated with the same detected/undetected NDVI trend would be compared with each other through hypothesis tests such as ANOVA, Kolmogorov-Smirnov (KS) and Anderson-Darling (AD) test. Thus, effects of various land cover types and elevation on NDVI trend would be distinguished. In addition, correlation between NDVI trend magnitude and land cover and elevation is evaluated with Spearman rank correlation analysis. In view of the vital roles of climatic factors during vegetation growth, the impacts of precipitation and temperature change in affecting the dependency of NDVI change trend on land cover and elevation are further identified through exploring partial correlation based on the Spearman rank correlation coefficient.

2.3.1. Seasonal MK trend test

The SMK test was proposed as an extension of the nonparametric Mann-Kendall (MK) test (Hirsch and Slack, 1984; Hirsch et al., 1982). Through performing MK test on individual seasons of the year, the overall $\overline{S}$ test statistic for SMK is computed as follows.

$$\overline{S} = \sum_{g=1}^{m} S_g \tag{1}$$

$$S_g = \sum_{i=1}^{n-1} \sum_{j=i+1}^{n} \mathrm{sgn}(X_{jg} - X_{ig}), \quad g = 1,2, ..., m \tag{2}$$

In which, S_g is statistic S for the gth season; m and n are the numbers of seasons and data in the season, respectively; X_{ig} stands for the value at the ith data for the gth season; sgn is the symbol function, which is expressed by using the following equation.

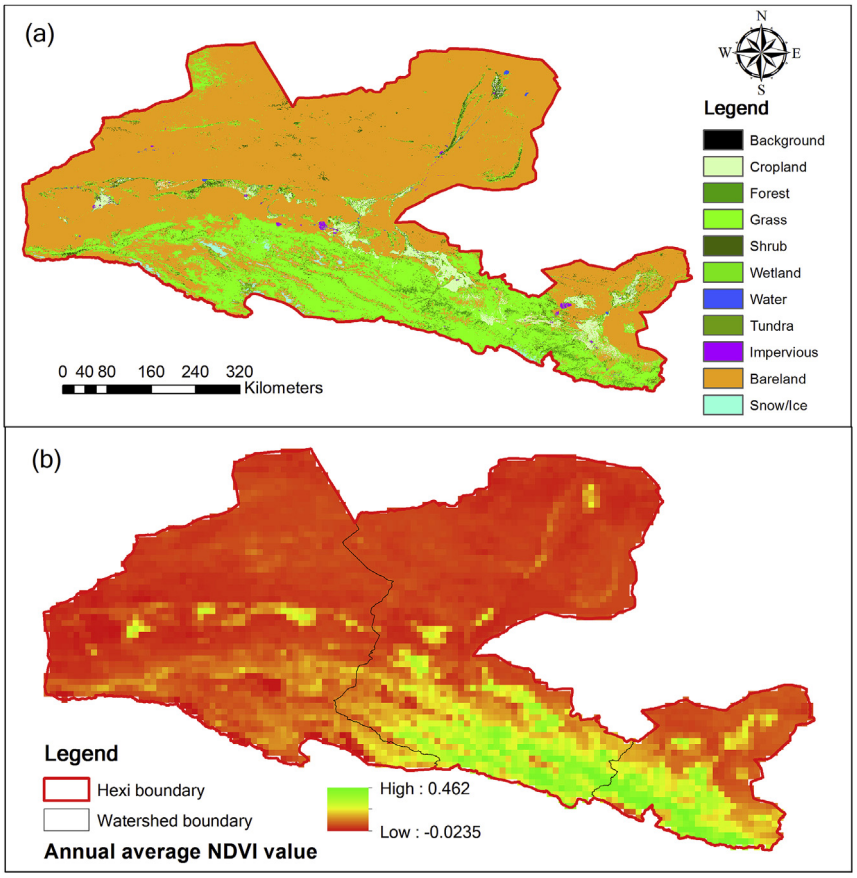

Fig. 2. Distribution of land cover (a) and mean annual NDVI values 1981 to 2015 (b) across the study area.

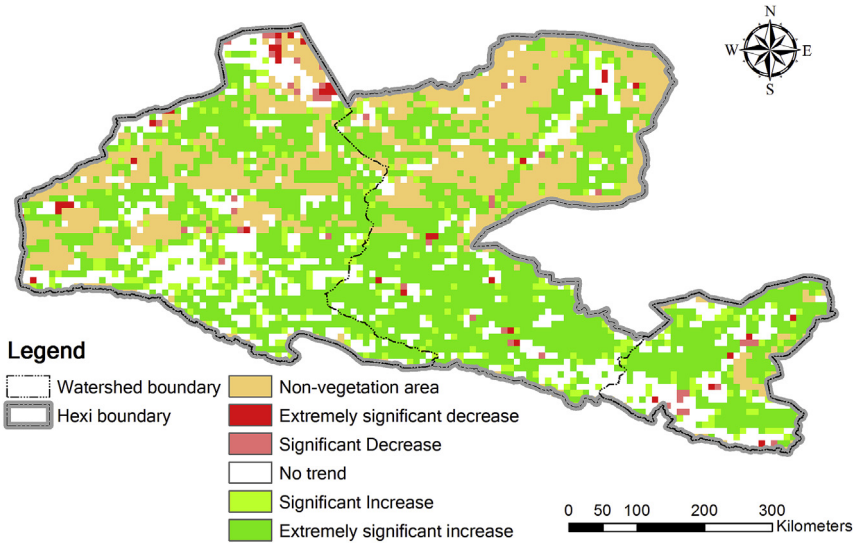

Fig. 3. SMK tests of NDVI change trends for the period 1981–2015 across the Hexi region.

$$\mathrm{sgn}(x) = \begin{cases} 1 & \text{if } x > 0 \\ 0 & \text{if } x = 0 \\ -1 & \text{if } x < 0 \end{cases} \tag{3}$$

When the product of m and n is more than 25, the distribution of $\overline{S}$ can be approximated by a normal distribution with expectation equal to the sum of the expectations of S_g under the null hypothesis ($\mu_{Sg} = 0$), and variance equal to the sum of their variances. Hence, $\overline{S}$ is standardized using:

$$Z_{\overline{S}} = \begin{cases} \frac{\overline{S}-1}{\sigma_{\overline{S}}} & \text{if } \overline{S} > 0 \\ 0 & \text{if } \overline{S} = 0 \\ \frac{\overline{S}+1}{\sigma_{\overline{S}}} & \text{if } \overline{S} < 0 \end{cases} \tag{4}$$

$$\text{where } \sigma_{\overline{S}} = \sqrt{\sum_{i=1}^{m} (n_i/18)\cdot(n_i - 1)\cdot(2n_i + 5)}. \tag{5}$$

The null hypothesis that there is no trend in the series is rejected at

Table 1
Characteristics of land cover and elevation in the three watersheds.

Items		Shule river watershed	Heihe river watershed	Shiyang river watershed
Land cover (%)	Shrub	1.91	3.03	3.74
	Crop	0.93	3.82	7.26
	Forest	0.004	0.94	2.58
	Grass	21.99	34.47	36.53
	Impervious	0.15	0.32	0.57
	Bare land	49.43	56.40	42.07
Elevation (m)	Average	1821.29	1409.63	1832.44
	Standard deviation	76.16	71.05	75.80

significance level α if $Z_{\bar{S}} > Z_{crit}$, where Z_{crit} is the value of the standard normal distribution with a probability of exceedance of $\alpha/2$.

2.3.2. Sen's slope estimation

The Sen's slope is estimated as the median of the linear change rates between two points in the data series. Similarly, the seasonal Sen's slope is calculated as the median of d_{ijk} for various seasons (Hirsch et al., 1982).

$$d_{ijk} = \frac{X_{ij} - X_{ik}}{j - k} \tag{6}$$

In which, $1 \le k < j \le n_i$, and n_i is the number of data in the ith season.

2.3.3. Kolmogorov-Smirnov and Anderson-Darling test

Regarding differences of two datasets, the hypothesis test would be useful to judge whether two datasets are drawn from the same parent population. As two typical kinds of nonparametric hypothesis test, both KS and AD test are based on the empirical distribution function (EDF) and have the advantage of making no assumption about the distribution of data (Stephens, 1974). The two-sample KS statistic is calculated by using:

$$D_{nn'} = \sqrt{\frac{n \cdot n'}{n + n'}} \sup_x |F_n(x) - F_{n'}(x)| \tag{7}$$

where $F_n(x)$ and $F_{n'}(x)$ are two empirical cumulative distribution values at x based on datasets with the size of n and n′, respectively; $\sup_x$ is the supremum of the set of distances. The null hypothesis that two datasets come from the same underlying distribution is rejected if $D_{nn'}$ is greater than the critical value D_α at a significance level of α. In the case of the simplicity of the *KS* test, it would lead to incorrect probabilities and inapplicable conclusions if it is not sensitive in establishing distances between two distributions. To address such a dilemma, the *KS* statistic test could be confirmed with bootstrap resampling, which can provide correct coverage even when the distributions being compared are not entirely continuous (Diamond and Sekhon, 2012)). Besides, the *AD* test is developed to compare datasets with the most prominent differences in near beginning or end of the EDF distributions, and is very sensitive when the EDFs cross each other many times with the deviation between the distributions being reduced (Scholz and Stephens, 1987). In addition, the *AD* test can perform the hypothesis test that whether k independent samples with sample sizes n_1, n_2, n_3, …, n_k arise from a common unspecified distribution function. The k-sample AD statistic generalizes to the following formula:

$$AD = \frac{n - 1}{n^2 \cdot (k - 1)} \sum_{i=1}^{k} \left[\frac{1}{n_i} \sum_{j=1}^{L} h_j \cdot \frac{(n \cdot F_{ij} - n_i \cdot H_j)^2}{H_j(n - H_j) - n \cdot h_j/4} \right] \tag{8}$$

where n denotes the number of the combined samples Z_n, z_j is the jth ordered value in Z_n ($j = 1, 2, 3, \ldots, L, L \le n$), h_j represents the number of data values in Z_n equal to z_j, H_j is the number of values in Z_n less than z_j, plus one half the number of values equal to z_j, and F_{ij} is the number of values in the ith sample which are less than z_j, plus one half the number of values in this sample which are equal to z_j.

In this study, the bootstrap versions of *KS* and *AD* test are employed, and the number of the bootstrap resampling is set as 2000.

2.3.4. Spearman rank correlation and partial correlation

Spearman rank correlation is usually used as a non-parametric alternative to linear regression and correlation because it applies ranks instead of assumptions about the distributions of the two variables. It works by calculating Pearson's correlation on the ranked values of data of interest. Hence, Spearman correlation coefficient is a statistical measure of the strength of a monotonic relationship between paired data.

In order to discover the link strength between two data sets while controlling the effect on one or more other continuous variables, partial correlation would provide the measure of the degree of association between two random variables after eliminating the influences of control variables (Tibshirani, 1996). A partial correlation coefficient can be written in terms of simple correlation coefficients, and $r_{XY|Z}$ stands for the Spearman rank correlation between X and Y after excluding the effect of Z. which is calculated as follows.

$$r_{XY|Z} = \frac{r_{XY} - r_{XZ} r_{YZ}}{\sqrt{(1 - r_{XZ}^2) \cdot (1 - r_{YZ}^2)}} \tag{9}$$

In addition, the hypothesis test would perform on the correlation coefficient to deduce the dependence in the change direction of two variables.

3. Results

3.1. Spatial distribution of NDVI trend

In the case of monthly NDVI at pixel level, about 70% of the vegetation area presents a significantly increasing trend in comparison with 2.85% and 27.18% for significantly decreasing trend and no trend, respectively. In addition, the hypothesis tests for 85.1% of pixels with an increasing trend are extremely significant ($P < 0.01$). Thus, positive change is the overall trend of vegetation cover during growth season across the Hexi region. According to Fig. 3, decreasing trends of NDVI only occurred at sparse pixels, which are mainly distributed in the north part of the Shule river watershed. In the contrast, pixels with an increasing trend were evenly distributed and more likely to be aggregated at the three watersheds.

Fig. 4 shows the overall NDVI time series of vegetation cover at the watershed level during growing season. Similar periodical changes would be observed with regards to the intra-annual variations of monthly NDVI values at the Shule, Shiyang and Heihe river watershed. The maximum NDVI value was obtained in July or August at the watersheds. From the east to west, moreover, NDVI value was reduced along with increasing area of desert landscape and bare land. Compared to apparent change for the Shiyang river watershed, change amplitudes of monthly NDVI value within one year for the Shule and Heihe river watershed were small, particularly for the Shule river watershed. According to the linear regression, the monthly NDVI value exhibits a positive linear change for all the three watersheds, the magnitude of which decreases gradually from east to west in accordance with the Shiyang, Heihe and Shule river watersheds. It was worth mentioning that the overall NDVI change trend at the Shiyang river watershed is statistically significant at $P < 0.1$.

3.2. Impacts of land cover and elevation variations on NDVI trend

The empirical distributions of land cover and elevation for three groups of pixels with no, increasing and decreasing change trends in monthly NDVI are shown in Fig. 5. The resulting shapes present varying

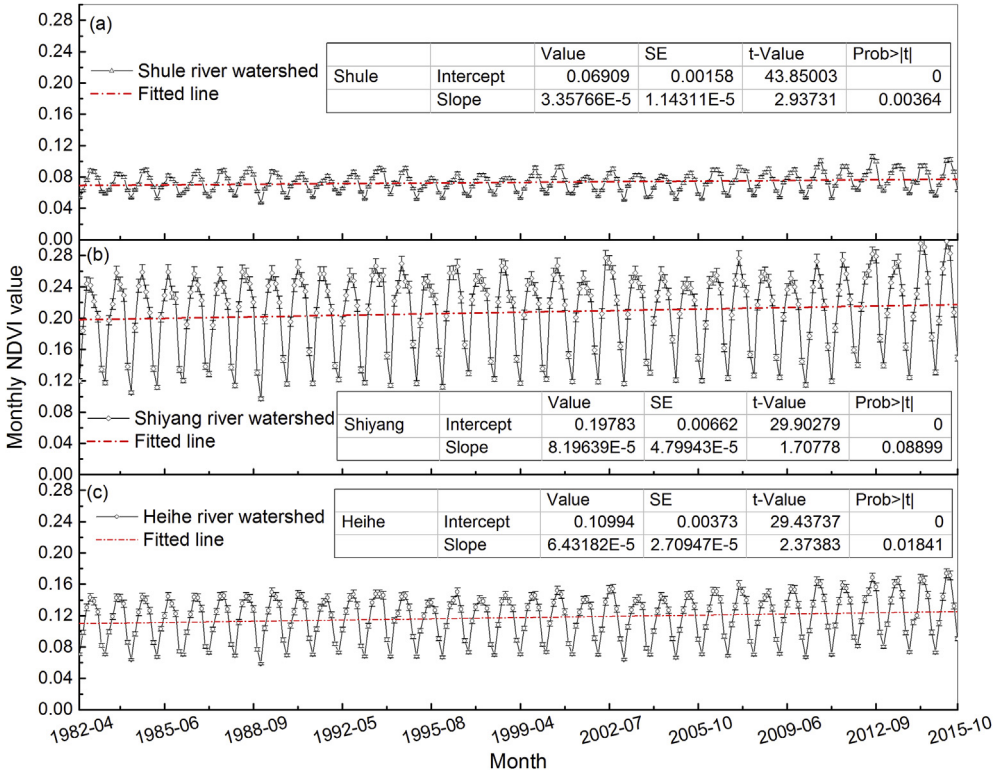

		Value	SE	t-Value	Prob>|t|
Shule	Intercept	0.06909	0.00158	43.85003	0
	Slope	3.35766E-5	1.14311E-5	2.93731	0.00364

		Value	SE	t-Value	Prob>|t|
Shiyang	Intercept	0.19783	0.00662	29.90279	0
	Slope	8.19639E-5	4.79943E-5	1.70778	0.08899

		Value	SE	t-Value	Prob>|t|
Heihe	Intercept	0.10994	0.00373	29.43737	0
	Slope	6.43182E-5	2.70947E-5	2.37383	0.01841

Fig. 4. Monthly NDVI value time series of the Shule, Shiyang and heihe river watershed.

characteristics with regards to land cover percentage and average elevation as well as standard variance of elevation. Both the crop and impervious land covers seem to play a meaningless role in NDVI change trend as a result of small area percentages. As illustrated in Fig. 6, each pair of pixel groups with different trends in NDVI was tested using repeated measures ANOVA and post hoc Tukey HSD tests, and as for symbols above different columns in each panel, no same letter existing implies that the differences of mean values of land cover percentage or elevation are statistically significant at $P < 0.05$. As a result, except for the crop and impervious land, there exist to be significant differences in

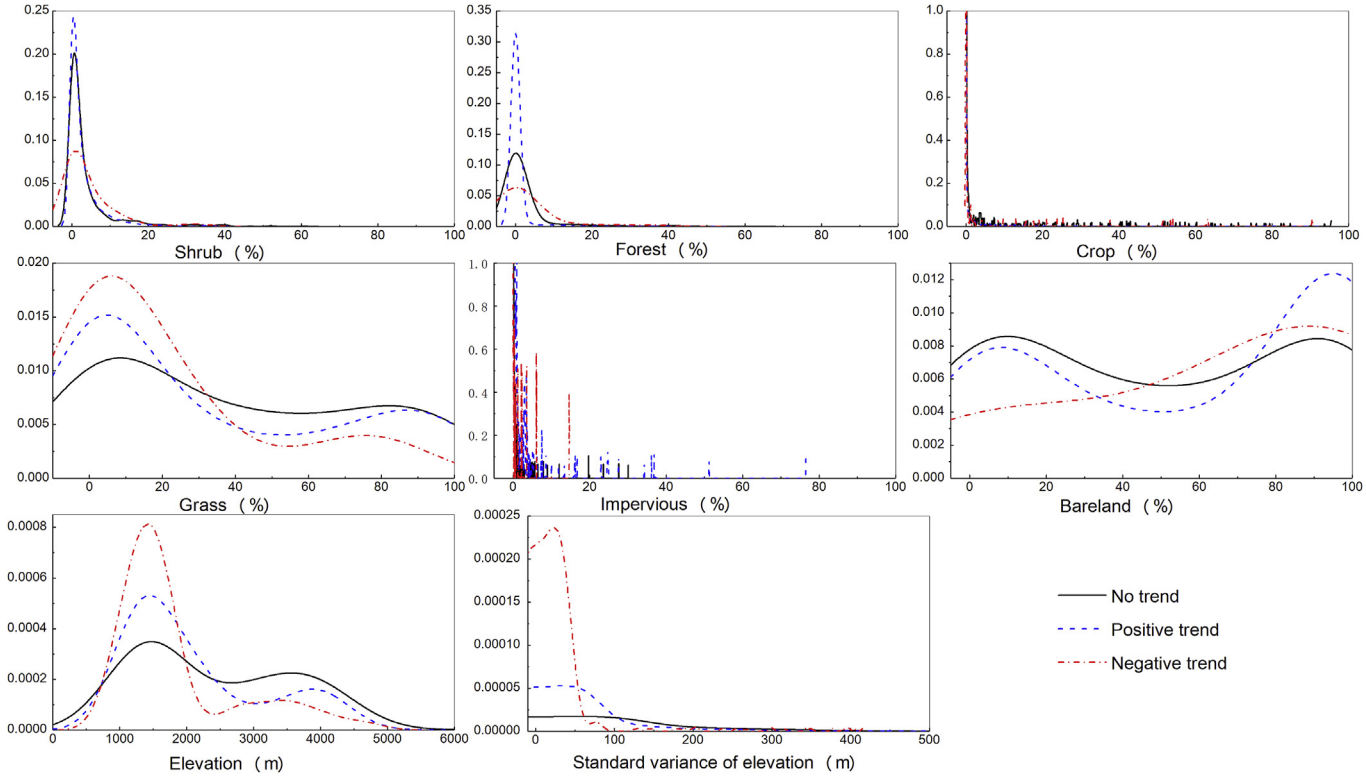

Fig. 5. Empirical distributions of land cover and elevation for pixels with various NDVI trends.

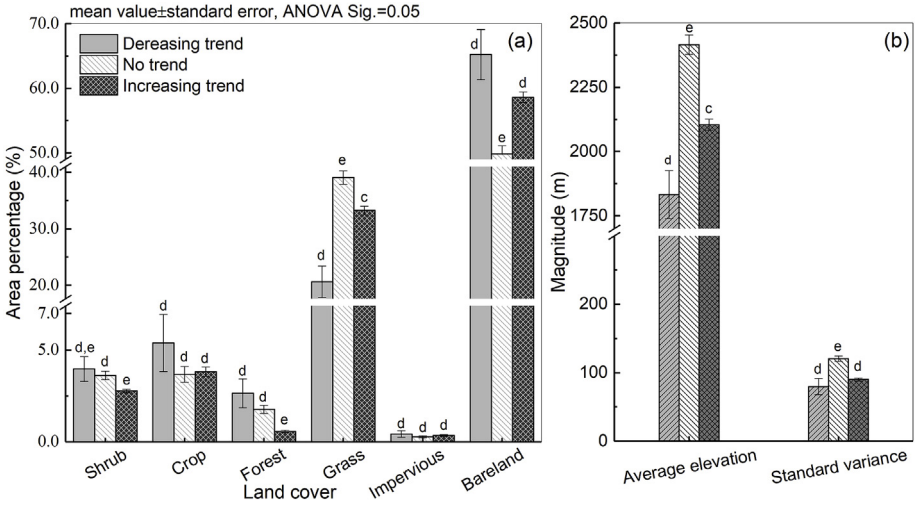

Fig. 6. ANOVA tests on land cover and elevation for pixels with various NDVI trends.

the land cover and elevation features. Besides, NDVI pixels with an increasing trend have significant differences in the average area percentages of shrub, forest, grass and bare land in comparison with those with no trend. In addition to such land cover as grass and bare land, the average elevation as well its standard variance exhibit significant differences between the pixel groups with a decreasing trend and no trend. As far as pixels with opposite trends are concerned, significant differences exist only in the forest, grass land and average elevation. In the meanwhile, the NDVI trend is more likely to be statistically significant for the pixels with low average elevations and less grassland but more bare land.

Comparisons of empirical distribution based on KS and AD tests were simultaneously implemented as shown in Table 2. The probability level below 0.05 would indicate a significant difference in the empirical distributions. Generally, the obtained results based on these two tests lead to non-consistent conclusions on distribution difference of land cover or elevation for different trend groups. For example, the distribution difference of shrub was not found to be significant between decreasing and no trends (NN) based on KS tests, while AD tests proved to be significant. Similar phenomenon could also be found between increasing and decreasing trends (PN) for forest, as well as between increasing and no trends (PNo) for crop. Regardless of varying statistic values, grassland was found to be the most sensitive type of land cover as it shows significant differences in the empirical distributions of area percentage associated with various NDVI change trends. Also, both the average value and standard variance of elevation present significant differences, indicating its essential role in influencing the growth conditions of vegetation as well as the NDVI value. Using AD tests to simultaneously analyze the differences of empirical distributions among various NDVI change trends (PNN), the elevation and almost all the land cover but crop were found to be statistically significant ($P < 0.05$). Therefore, distinct characteristics of land cover and elevation concerning various trends would further reveal the dependency of NDVI change trend on land cover and elevation.

Table 2
KS and AD tests on land cover and elevation distribution for pixels with various NDVI variation trends.

Item	Kolmogorov-Smirnov test (nboots = 3000)			Anderson-Darling test (exact)			
	NN	PNo	PN	NN	PNo	PN	PNN
Shrub	***0.12***	0.02	***0.12***	0.03	0.046	***0.051***	0.004
Crop	***0.57***	***0.06***	***0.96***	***0.33***	0.006	***0.38***	***0.38***
Forest	***0.91***	0.00	***0.19***	***0.66***	0.001	0.009	0.00
Grass	0.00	0.00	0.00	0.00	0.00	0.002	0.00
Impervious	***0.95***	0.04	***0.66***	***0.64***	0.039	***0.30***	0.007
Bare land	0.00	0.00	0.05	0.00	0.00	***0.22***	0.00
Average elevation	0.00	0.00	0.00	0.00	0.00	0.004	0.00
Standard variance of elevation	0.00	0.00	0.00	0.00	0.00	0.003	0.00

The bold and italic intends to distinguish tests ($P > 0.05$) from the others ($P \leq 0.05$) by the significance level.

3.3. Relations between NDVI trend magnitude and land cover and elevation

Fig. 7 shows the distribution of Sen's slope for monthly NDVI values, and the circle mark on a pixel implies that no significant trend in NDVI was detected. No matter whether the trend is statistically significant, most of the Hexi region indicates a positive magnitude of the NDVI change based on the positive SS value. In the meanwhile, the magnitude seems to decrease mainly along with the direction from east to west. Although negative Sen's slopes of NDVI were only revealed for several discrete pixels, the magnitudes were too pronounced to neglect, especially for the red pixels in the south of the Shiyang and Heihe river watersheds (Fig. 7). Besides, the southeast of the Hexi region was simultaneously subjected to high magnitudes of both positive and negative NDVI change trends.

As shown in Fig. 8, NDVI trend magnitude is presented against the area percentage of each land cover type. Pixels with a significant trend and no trend are denoted as red and grey dots. According to linear regression analysis, all types of land cover but impervious land impose significant impacts on the change magnitude of NDVI. Moreover, increasing land covers of shrub, crop, grassland and forest would contribute to the NDVI trend magnitude, but no significant correlation is revealed between forest and Sen's slope for NDVI pixels with no significant trend. In addition, Sen's slope seems to be more susceptible to land cover types such as crop, shrub and forest than grassland, since 10% increase of grassland area percentage would only result in an increase of Sen's slope for significant NDVI trend by 7.846×10^{-5} per year, while 10% increase in the crop land area percentage would lead to about 2.440×10^{-4} increase in the Sen's slope for significant NDVI trends (Fig. 8b). This contribution of crop to the NDVI change would be mainly from anthropogenic activities such as farming practice and irrigation (Yang et al., 2016), and intentional human cultivation of crop land would favor positive direction of vegetation growth as well as NDVI change. However, it is still worth noting that contribution to NDVI change from shrub, crop and forest might be small due to their low area percentage and discrete distribution compared to that of

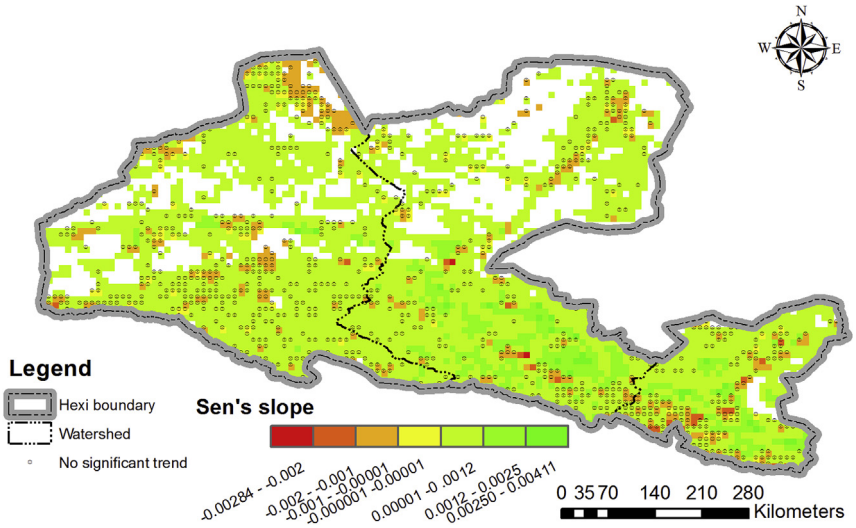

Fig. 7. Distribution of Sen's slope for monthly NDVI values across the Hexi region.

grassland. In the contrast, increasing bare land would lead to Sen's slope decrease for NDVI variations, consistent with its effects on NDVI value. Moreover, the Sen's slopes for NDVI change and temperature would increase in accordance with elevation based on the significant correlation (Fig. 8g, h and l). Although the change direction of precipitation is positive, the high elevation area has a low value of Sen's slope for significant trend of precipitation.

3.4. Comparisons of NDVI trend with temperature and precipitation

Considering the importance of climatic factors in regulating vegetation growth, trend analysis on precipitation and air temperature was further performed across the Hexi region. Fig. 9 shows the distribution of Sen's slope for precipitation and temperature during the growing season. An increasing trend of air temperature was revealed at most of the pixels, and the obtained distribution of Sen's slope presents a very similar pattern with the annual average NDVI. In particular, air temperature increase seems to be more apparent in the south of the Hexi Region, in which vegetation cover grows better. In the contrast, precipitation increase occurs mainly in the east of the Hexi region. Although positive trends were also indicated in the middle of the Shule river watershed and in the northeast of the Heihe river watershed, the increasing magnitude of precipitation is found to be relatively low. Through comparing the spatial distribution of NDVI with precipitation

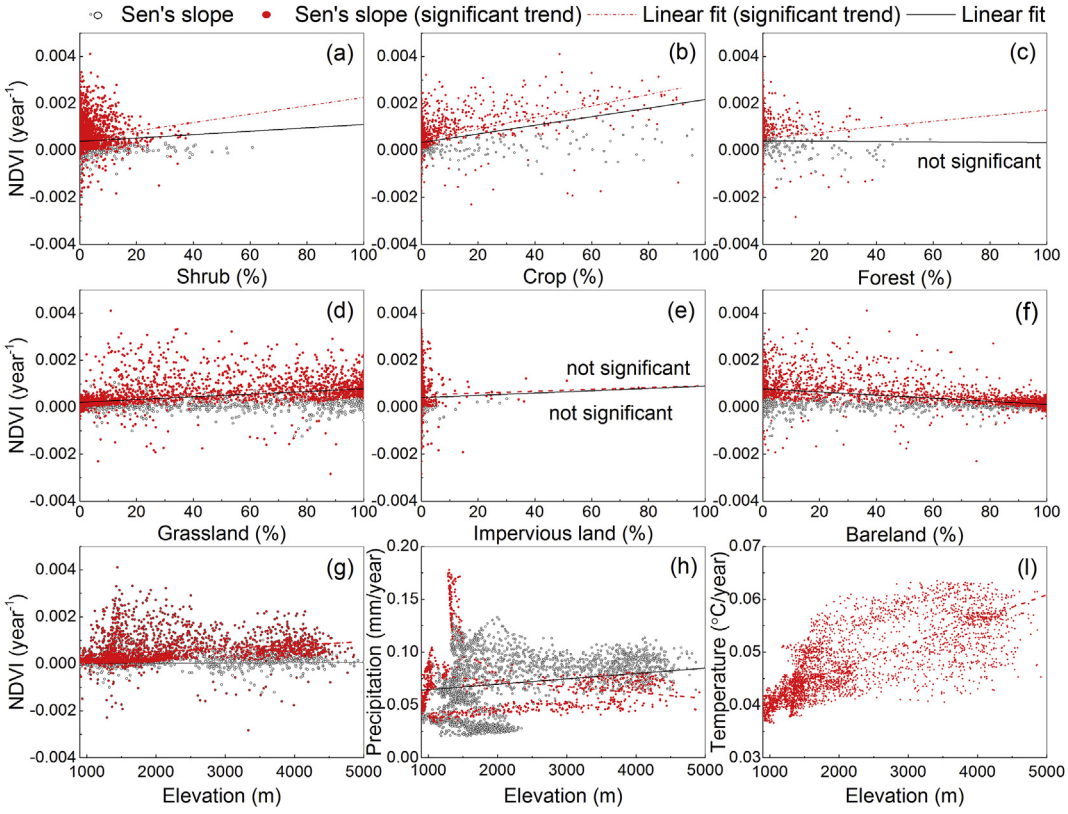

Fig. 8. The Sen's slope of NDVI against land cover area percentage and elevation (a ~ g), and precipitation and air temperature against the elevation (h & l).

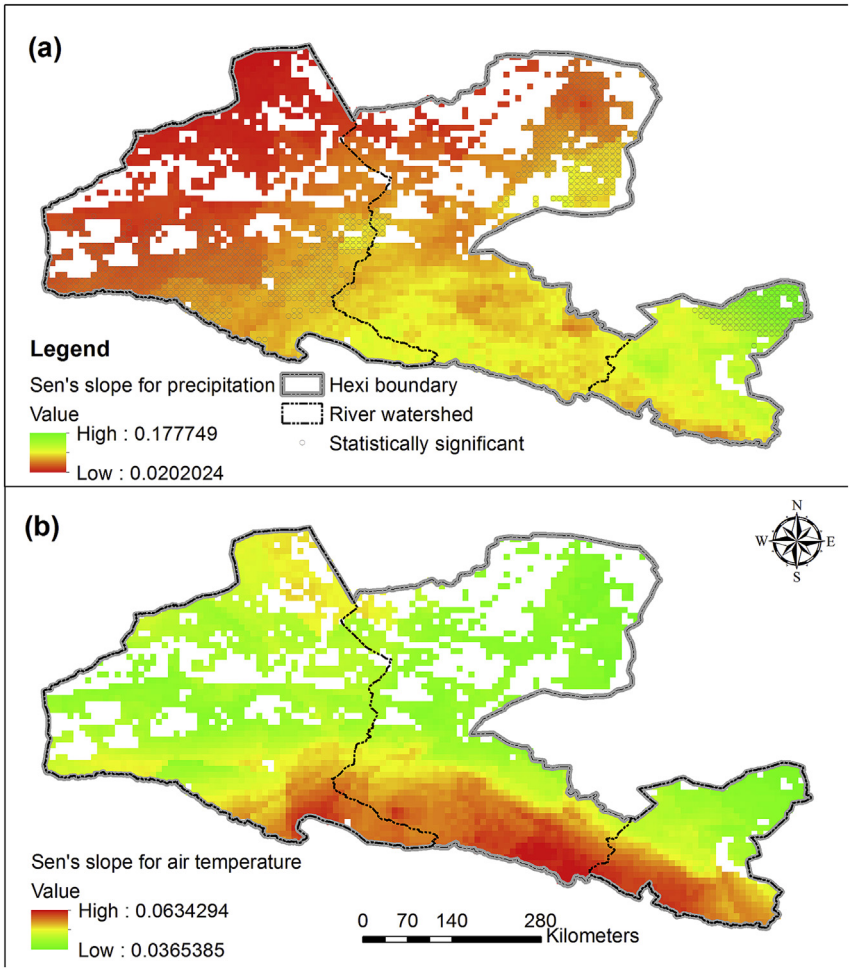

Fig. 9. Spatial distribution of Sen's slope for precipitation and air temperature during growing season across the Hexi region.

and temperature, there exist to be non-consistent patterns associated with significant trends and change magnitude. For further analysis, it would confirm the roles of changing underlying conditions with high spatial heterogeneity and various influences of human activities such as crop rotation and water diversion for irrigation (Wang et al., 2003).

Based on the analysis of relations between elevation and NDVI, precipitation and temperature at pixel level, elevation as well as its variance have various effects on Sen's slopes for NDVI, precipitation and air temperature. Pixels with significant trends were denoted by circles in the contour map (Fig. 10). As mentioned above, relatively level pixels with low average elevation are more likely to present a significant NDVI trend, and such trend mainly occurred at pixels with average elevation below 2500 m, along with standard variance of elevation below 200 m (Fig. 10a). However, increasing magnitudes of precipitation and air temperature at these pixels are relatively small (Fig. 10b and c). In contrast with a significant trend of air temperature across the whole region, pixels with a significant trend of precipitation are scattered at various terrain levels.

When NDVI trend magnitude against precipitation and air temperature is concerned, the detected NDVI trends were mainly found in areas with increasing magnitude of precipitation < 0.06 mm/year or temperature < 0.05 °C/year (Fig. 10d). Although no significant trend was detected, there exists to be a concentrated area with high values for increasing magnitude of NDVI corresponding to precipitation and temperature trend magnitude of ~0.15 mm/year and ~0.05 °C/year, respectively (Fig. 10d). Consequently, positive changes of precipitation and temperature are generally beneficial to positive change trend in vegetation growth, but increasing change magnitudes of precipitation and temperature would not lead to increasing Sen's slopes for NDVI, which would further indicate the dependency of NDVI variations on other factors.

4. Discussion

4.1. Variations in NDVI trend over the Hexi region

A significantly positive trend in the growth season NDVI was observed in major parts of the Hexi region as demonstrated in other literatures. Guan et al. (2018) revealed an upward trend in over 90% of the Hexi corridor when inter-annual variations in NDVI was investigated for period 2000–2015. Note that the MODIS NDVI data at 500 m spatial resolution in the study of Guan et al. (2018) was considered with a short period. Our work suggested a significantly increasing trend in ~70% of the vegetated area during 1983–2015. Such inconsistencies in detected areas would result from different data sources and investigation periods. In addition, seasonal variations in NDVI were considered in our study, while the work of Guan et al. (2018) focused on annual maximum NDVI. The calculations based on different NDVI pixel resolutions would further lead to statistical differences. Yang et al. (2016) demonstrated that the average $NDVI_{max}$ showed an increasing trend at the rate of 0.65×10^{-3}/a during 1982–2013 in desert vegetation, which occupied about 50% of the Hexi region. The revealed areas with increasing and decreasing trend accounted for 40.51% and 5.69%, respectively. In the meanwhile, the significant increases of $NDVI_{max}$ mainly appeared in the typical desert vegetation according to Yang et al. (2016). It is consistent with our

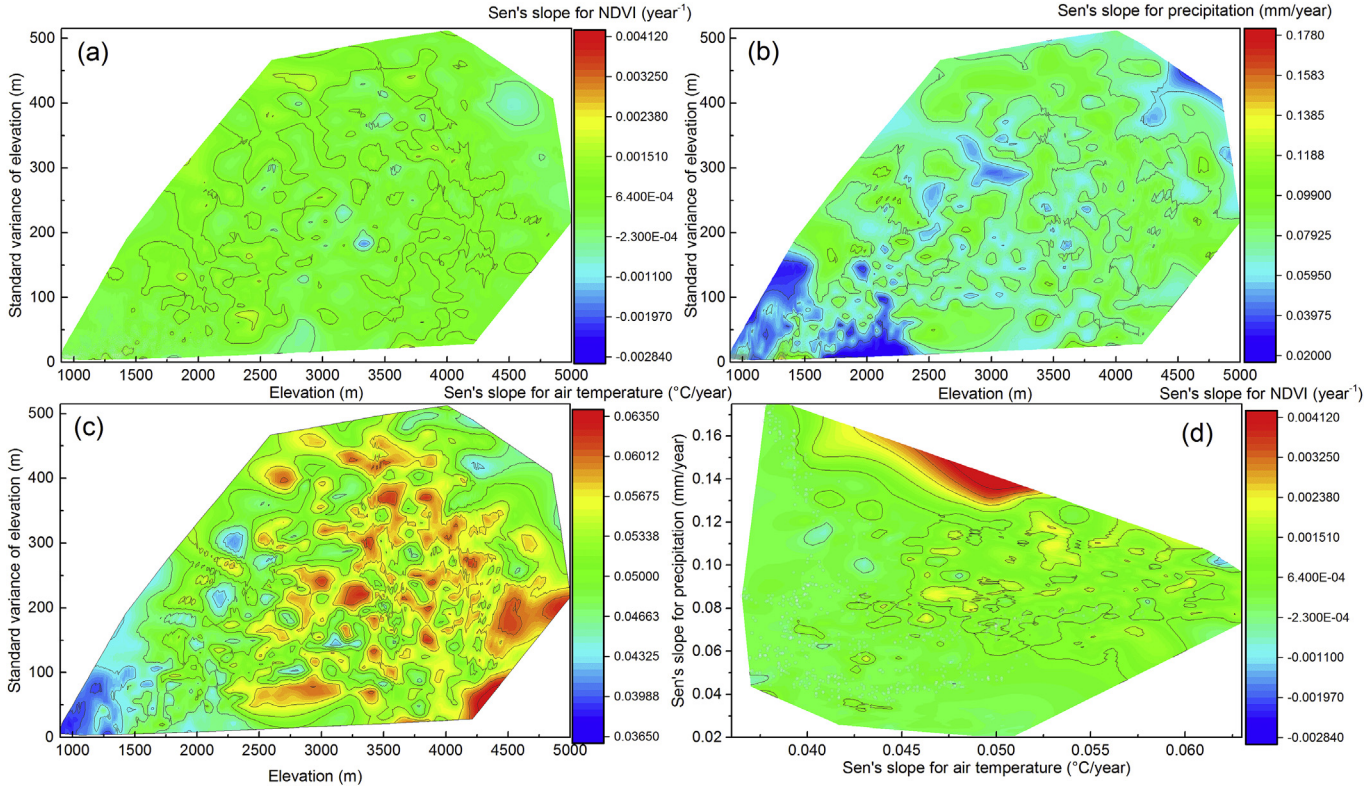

Fig. 10. Effect of elevation on the relation between NDVI trend, precipitation and temperature.

finding that the identified areas with a significant trend were generally occupied by less grass but more bare land. Guan et al. (2018) also concluded that more arid area's vegetation experienced a temporal shift in greening as temperature significantly increased for period 2000–2015.

4.2. Effects of climate change on the relation between NDVI trend and land cover and elevation

Previous studies mostly agreed that precipitation is the key climatic factor for vegetation growth based on partial correlation analysis and multiple linear regression analysis (Guan et al., 2018; Yang et al., 2016). However, the conclusions were built on the analysis of NDVI and temperature and precipitation at annual scale, the implications of climate change on NDVI trend were not clearly revealed. As demonstrated in Fig. 11, Spearman rank correlation analysis was applied to partition effects of precipitation and temperature trend change on the relations between Sen's slope for variations in NDVI and land cover and elevation. Four scenarios on the Spearman rank correlation were analyzed. According to correlation coefficients under consideration of precipitation and temperature, both elevation and land cover excluding bare land have a significantly positive correlation with NDVI, especially grass land. As effects of precipitation and temperature were ignored, the correlations between NDVI and elevation and land cover present various responses. Generally, the absolute values of correlation coefficients become smaller, but the correlation changes from positive to negative for both elevation and forest. Apparently, precipitation and temperature change would impose pronounced effects on the dependency of NDVI trend on land cover and elevation. Although precipitation affects water availability to vegetation growth, while temperature determines the vegetation growth stages under natural conditions. Previous studies showed a positive correlation between NDVI and annual precipitation (Yang et al., 2016), but different roles were played by air temperature and precipitation change in affecting the change trends in vegetation growth.

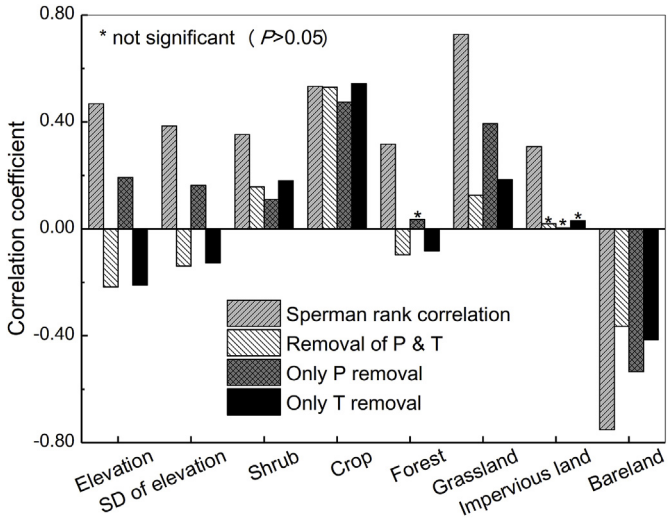

Fig. 11. Spearman rank correlation between Sen's slope of NDVI and elevation and land cover with/without the consideration of variations in precipitation and temperature.

It is interesting that similar results of correlation coefficient were obtained with consideration of only precipitation and without consideration of precipitation and temperature (Fig. 11). According to the variations in coefficients, effects of air temperature might be more prominent than those of precipitation on influencing the dependency of NDVI trend on underlying surface conditions. However, such effects of air temperature would be different when elevation and various types of land cover are concerned. According to correlation coefficient with consideration of both temperature and precipitation, shrub and crop land covers are more sensitive to precipitation change than temperature change. Besides, very slight changes of correlation coefficient under four scenarios would suggest that the NDVI variations from crop might

not be very vulnerable to changes of both temperature and precipitation. It is consistent with conclusions by Yang et al. (2016) that desert vegetation in the lower reaches of Shiyang and Shule river basins may be mainly controlled by human activities. Based on correlation coefficients for different scenarios, the correlation between NDVI trend magnitude and average elevation is very similar with that between NDVI trend magnitude and variance of elevation. In comparison with precipitation, moreover, temperature plays a distinct part in affecting the dependency of NDVI trend on elevation. Similarly, the correlation between NDVI trend magnitude and forest cover is more subjected to air temperature change. Compared to the other land types, contribution of the grass to NDVI trend magnitude is very sensitive to temperature change. In addition, effects of precipitation change would be positive on the contribution of grassland to change trend for NDVI variations. However, increasing bare land area would lead to adverse effects on NDVI trend magnitude. Given the above, the ultimate NDVI trend was a result of complex interactions between climate change, human activities, and land cover/elevation characteristics.

4.3. Adaptability of vegetation growth to increasing air temperature

Based on our recent studies on the monthly terrestrial water storage (*TWS*) anomaly data through Apirl 2002 to March 2016, the Hexi region experienced a significant decrease in the *TWS* by 1.3 mm/yr (linear regression, $P < 0.05$). Such dramatic changes would no doubt lead to extremely adverse effects on the ecological integrity. However, what would be reasonable explanations for increasingly improved vegetation growth for past thirty years? On the one hand, large uncertainties might exist in the remotely sensed data across the Hexi region, which might give rise to wrong conclusions on decrease in *TWS* at the concerned region. On the other hand, the increasing melted water would favor the improvement of vegetation growth from the glaciers in high-elevation mountain areas due to temperature increase (Zhang et al., 2016). Note that changes of *TWS* comprise of water components of snow water, groundwater, soil water and surface water. Thus, changes in actual water availability to vegetation would need further analysis of water balance to gain insights into vegetation change trend, although precipitation change was found to have a positive effect on vegetation change (Long et al., 2015).

The water use efficiency (WUE) measures the trade-off between carbon gain and water loss of terrestrial ecosystems, and to understand its dynamics would help better predict ecosystem responses to climate change (Liu et al., 2015). Based on our recent work, the ecosystem-level WUE (expressed as monthly gross primary productivity (GPP)/evapotranspiration (EVAP)) across the Hexi region showed no significant change trends from 2000 to 2014. As a result of the limits of available dataset, monthly WUE calculations were only obtained for period 2000–2014. Also, no significant trends were detected in both GPP and EVAP. Taking the significantly increasing air temperature into consideration, how vegetation growth adapts to such changes in this arid/semi-arid region? As suggested by Liu et al. (2015), ecosystem–level WUE could consider the effects of temperature (T) through changing the expression as: WUE = (GPP/T) * (T/EVAP). In which, GPP/T measures how much dry matter was produced through plant transpiration, while T/EVAP implies that how water vapor flux is allocated between ecosystem biological and physical processes. According to SMK test results, the time series of GPP/T and T/EVAP for the entire region show a significant increasing trend (Fig. 12), both of which would promote the carbon gain of vegetation. Thus, the positive change trends for NDVI in vegetated areas would benefit from the ecosystem adaptability through increasing vegetable activity at grassland and oasis areas of the Hexi region (Zhao et al., 2012). The increasing air temperature was considered to slow down the degradation of leaf chlorophyll and enhance photosynthesis in temperature-limited regions (Piao et al., 2006). Based on the correlation analysis and adaptability of vegetation, the change trend for NDVI variations across the Hexi region would be mainly dominated by grass land, vegetable activity of which would increase as a result of significantly increasing air temperature. Precipitation change would enhance the dependency of NDVI change trend on shrub and crop land through improving water availability, but crop land was found to be insensitive to both temperature and precipitation change, implying that the vegetation change at crop land might be mainly caused by human activities.

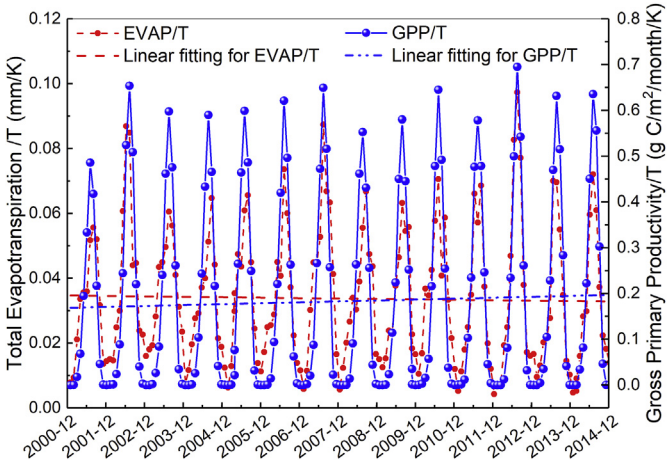

Fig. 12. Monthly changes of GPP/T and EVAP/T from 2000 to 2014.

5. Conclusions

Based on the GMMIS NDVI 3g.v1 dataset, the trend in monthly NDVI values during growing season (April to October) from 1982 to 2015 was examined as well as its dependency on elevation and land cover across the Hexi region. The summarized conclusions are given as follows.

(1) NDVI was generally reduced along with increasing area of desert landscape and bare land from east to west in accordance with the Shiyang, Heihe and Shule river watersheds. The monthly NDVI value during vegetation growth period presented a positive linear change for the three watersheds. Multiple hypothesis tests revealed the differences of underlying surface characteristics of land cover and elevation with respect to three groups of pixels associated with increasing, decreasing and no trends in NDVI. As two dominant types of land cover, the grass and bare land played a critical part in NDVI trend. In particular, variations in grassland cover would mainly account for variations in the detected trend, and the identified areas with a significant trend were generally occupied by less grass but more bare land. However, more bare land would reduce the NDVI trend magnitude. In the contrast, increasing land covers such as crop, shrub and forest would be favorable to improve the NDVI trend magnitude. Besides, increase in elevation would lead to slight increase in the magnitude of the NDVI trend, but the significant trend was mainly observed at areas with an average elevation below 2500 m and standard variance of elevation values at pixel level below 200 m. Furthermore, the interactions between elevation and land cover characteristics complicated the detected trend in NDVI as the type and distribution of land cover as well as climatic conditions were very vulnerable to variations in elevation for the Hexi region.

(2) Precipitation and temperature are important driving factors for the increasing NDVI trend over last thirty years, but responses of vegetation growth to the changes of precipitation and temperature rest upon spatial variations in land cover and elevation. Generally, air temperature change played a more prominent role in affecting NVDI trend than precipitation, especially for its dependency on

elevation, forestry and grassland. Yet, the crop and shrub land covers were more vulnerable to precipitation change relative to that of temperature, but the contribution of crop to NDVI change was considered to be mainly affected by human activities during last thirty years. No doubt that the environmental conservation and irrigation management schemes promoted by local government have improved the ecological conditions for vegetation growth. In order to adapt to increasing air temperature, besides, vegetable activity has been found to increase accordingly, especially for grassland cover. In the future, water availability to vegetation growth as well as the effects of land use/cover changes in the Hexi region would be urgently investigated. Again, analysis of uncertainties from data sources and methods should be also performed in order to gain more insights into vegetation changes.

Acknowledgement

This study was financially supported by the National Natural Science Foundation of China (Nos. 51809007 & 91647212) and the China Postdoctoral Science Foundation (2015M571048). The authors would also like to thank the editors and anonymous reviewers for their valuable comments and suggestions on the improvement of the manuscript.

References

Delhomme, J.P., 1978. Kriging in the hydrosciences. Adv. Water Resour. 1, 251–266.
Diamond, A., Sekhon, J.S., 2012. Genetic matching for estimating causal effects: a general multivariate matching method for achieving balance in observational studies. Rev. Econ. Stat. 95, 932–945.
Fang, S., Yan, J., Che, M., Zhu, Y., Liu, Z., Pei, H., Zhang, H., Xu, G., Lin, X., 2013. Climate change and the ecological responses in Xinjiang, China: model. simulations and data analyses. Quat. Int. 311, 108–116.
Gao, L., Zhang, Y., 2016. Spatio-temporal variation of hydrological drought under climate change during the period 1960-2013 in the Hexi Corridor, China. J. Arid Land 8, 157–171.
Gong, P., Wang, J., Yu, L., Zhao, Y., Zhao, Y., Liang, L., Niu, Z., Huang, X., Fu, H., Liu, S., Li, C., Li, X., Fu, W., Liu, C., Xu, Y., Wang, X., Cheng, Q., Hu, L., Yao, W., Zhang, H., Zhu, P., Zhao, Z., Zhang, H., Zheng, Y., Ji, L., Zhang, Y., Chen, H., Yan, A., Guo, J., Yu, L., Wang, L., Liu, X., Shi, T., Zhu, M., Chen, Y., Yang, G., Tang, P., Xu, B., Giri, C., Clinton, N., Zhu, Z., Chen, J., Chen, J., 2013. Finer resolution observation and monitoring of global land cover: first mapping results with Landsat TM and ETM+ data. Int. J. Rem. Sens. 34, 2607–2654.
Guan, Q., Yang, L., Pan, N., Lin, J., Xu, C., Wang, F., Liu, Z., 2018. Greening and browning of the Hexi corridor in northwest China: spatial patterns and responses to climatic variability and anthropogenic drivers. Rem. Sens. 10.
Hermance, J.F., Augustine, D.J., Derner, J.D., 2015. Quantifying characteristic growth dynamics in a semi-arid grassland ecosystem by predicting short-term NDVI phenology from daily rainfall: a simple four parameter coupled-reservoir model. Int. J. Rem. Sens. 36, 5637–5663.
Hirsch, R.M., Slack, J.R., 1984. A nonparametric trend test for seasonal data with serial dependence. Water Resour. Res. 20, 727–732.
Hirsch, R.M., Slack, J.R., Smith, R.A., 1982. Techniques of trend analysis for monthly water quality data. Water Resour. Res. 18, 107–121.
Jackson, R.D., Huete, A.R., 1991. Interpreting vegetation indexes. Prev. Vet. Med. 11, 185–200.
Liu, Y., Xiao, J., Ju, W., Zhou, Y., Wang, S., Wu, X., 2015. Water use efficiency of China's terrestrial ecosystems and responses to drought. Sci. Rep. 5, 13799.
Long, D., Longuevergne, L., Scanlon, B.R., 2015. Global analysis of approaches for deriving total water storage changes from GRACE satellites. Water Resour. Res. 51, 2574–2594.
Moreno-de las Heras, M., Diaz-Sierra, R., Turnbull, L., Wainwright, J., 2015. Assessing vegetation structure and ANPP dynamics in a grassland-shrubland Chihuahuan ecotone using NDVI-rainfall relationships. Biogeosciences 12, 2907–2925.
Murray, S.J., Watson, I.M., Prentice, I.C., 2013. The use of dynamic global vegetation models for simulating hydrology and the potential integration of satellite observations. Prog. Phys. Geogr. 37, 63–97.
Myneni, R.B., Hall, F.G., Sellers, P.J., Marshak, A.L., 1995. The interpretation of spectral vegetation indexes. IEEE Trans. Geosci. Rem. Sens. 33, 481–486.
Peng, S., Chen, A., Xu, L., Cao, C., Fang, J., Ranga, B.M., Jorge, E.P., Compton, J.T., Piao, S., 2011. Recent change of vegetation growth trend in China. Environ. Res. Lett. 6, 044027.
Pettorelli, N., Vik, J.O., Mysterud, A., Gaillard, J.M., Tucker, C.J., Stenseth, N.C., 2005. Using the satellite-derived NDVI to assess ecological responses to environmental change. Trends Ecol. Evol. 20, 503–510.
Piao, S., Ciais, P., Huang, Y., Shen, Z., Peng, S., Li, J., Zhou, L., Liu, H., Ma, Y., Ding, Y., Friedlingstein, P., Liu, C., Tan, K., Yu, Y., Zhang, T., Fang, J., 2010. The impacts of climate change on water resources and agriculture in China. Nature 467, 43–51.
Piao, S., Fang, J., Zhou, L., Ciais, P., Zhu, B., 2006. Variations in satellite-derived phenology in China's temperate vegetation. Global Change Biol. 12, 672–685.
Reed, B.C., Schwartz, M.D., Xiao, X., 2009. Remote sensing phenology: status and the way forward. In: Noormets, A. (Ed.), Phenology of Ecosystem Processes. Springer, New York, pp. 231–246.
Scholz, F.W., Stephens, M.A., 1987. K-sample anderson-darling tests. J. Am. Stat. Assoc. 82, 918–924.
Shi, Y., Shen, Y., Kang, E., Li, D., Ding, Y., Zhang, G., Hu, R., 2007. Recent and future climate change in northwest China. Climatic Change 80, 379–393.
Stephens, M.A., 1974. EDF statistics for goodness of fit and some comparisons. J. Am. Stat. Assoc. 69, 730–737.
Suding, K.N., Farrer, E.C., King, A.J., Kueppers, L., Spasojevic, M.J., 2015. Vegetation change at high elevation: scale dependence and interactive effects on Niwot Ridge. Plant Ecol. Divers. 8, 713–725.
Tao, J., Zhang, Y.J., Dong, J.W., Fu, Y., Zhu, J.T., Zhang, G.L., Jiang, Y.B., Tian, L., Zhang, X.Z., Zhang, T., Xi, Y., 2015. Elevation-dependent relationships between climate change and grassland vegetation variation across the Qinghai-Xizang Plateau. Int. J. Climatol. 35, 1638–1647.
Tibshirani, R., 1996. Regression shrinkage and selection via the lasso. J. Roy. Stat. Soc. B 58, 267–288.
Wang, G., Ding, Y., Shen, Y., Lai, Y., 2003. Environmental degradation in the Hexi Corridor region of China over the last 50 years and comprehensive mitigation and rehabilitation strategies. Environ. Geol. 44, 68–77.
Wang, H., Chen, A., Wang, Q., He, B., 2015. Drought dynamics and impacts on vegetation in China from 1982 to 2011. Ecol. Eng. 75, 303–307.
Wang, Y., Feng, Q., Chen, L., Yu, T., 2013. Significance and effect of ecological rehabilitation project in inland river basins in northwest China. Environ. Manag. 52, 209–220.
Wei, L., Feng, Q., Deo, R.C., 2018. Changes in climatic elements in the Pan-Hexi region during 1960-2014 and responses to global climatic changes. Theor. Appl. Climatol. 133, 405–420.
Yang, X., Liu, S., Yang, T., Xu, X., Kang, C., Tang, J., Wei, H., Ghebrezgabher, M.G., Li, Z., 2016. Spatial-temporal dynamics of desert vegetation and its responses to climatic variations over the last three decades: a case study of Hexi region in Northwest China. J. Arid Land 8, 556–568.
Yin, D., Li, X., Huang, Y., Si, Y., Bai, R., 2015. Identifying vegetation dynamics and sensitivities in response to water resources management in the heihe river basin in China. Adv. Meteorol. 2015, 12.
Yu, L., Wang, J., Li, X., Li, C., Zhao, Y., Gong, P., 2014. A multi-resolution global land cover dataset through multisource data aggregation. Sci. China Earth Sci. 57, 2317–2329.
Zeng, B., Zhang, F., Yang, T., Qi, J., Ghebrezgabher, M.G., 2018. Alpine sparsely vegetated areas in the eastern Qilian Mountains shrank with climate warming in the past 30 years. Prog. Phys. Geogr. Earth Environ. 42, 415–430.
Zhang, R., Ouyang, Z.-T., Xie, X., Guo, H.-Q., Tan, D.-Y., Xiao, X.-M., Qi, J.-G., Zhao, B., 2016. Impact of climate change on vegetation growth in arid northwest of China from 1982 to 2011. Rem. Sens. 8, 364.
Zhang, Y., Fu, G., Sun, B., Zhang, S., Men, B., 2015. Simulation and classification of the impacts of projected climate change on flow regimes in the arid Hexi Corridor of Northwest China. J. Geophys. Res. Atmos. 120, 7429–7453.
Zhao, X., Tan, K., Zhao, S., Fang, J., 2011. Changing climate affects vegetation growth in the arid region of the northwestern China. J. Arid Environ. 75, 946–952.
Zhao, X., Zhou, D.J., Fang, J.Y., 2012. Satellite-based studies on large-scale vegetation changes in China. J. Integr. Plant Biol. 54, 713–728.
Zheng, Y., Han, J., Huang, Y., Fassnacht, S.R., Xie, S., Lv, E., Chen, M., 2018. Vegetation response to climate conditions based on NDVI simulations using stepwise cluster analysis for the Three-River Headwaters region of China. Ecol. Indicat. 92, 18–29.